DEVELOPMENT OF SIMPLIFIED TEST METHOD WITH HPFRCC SCALED MODELS

NORIKO TOKUI[1)], YOSHIAKI NAKANO[2)], YASUSHI SANADA[3)], YUKI SAKAI[4)], HARUHIKO SUWADA[5)], and HIROSHI FUKUYAMA[6)]

[1)] Graduate School of Engineering, University of Tokyo, Tokyo 153-8505, Japan
Email: tokui@iis.u-tokyo.ac.jp
[2)] Institute of Industrial Science, University of Tokyo, Tokyo 153-8505, Japan
Email: iisnak@iis.u-tokyo.ac.jp
[3)] Earthquake Research Institute, University of Tokyo, Tokyo 113-0032, Japan
Email: ysanada@eri.u-tokyo.ac.jp
[4)] Institute of Engineering Mechanics and Systems, University of Tsukuba, Ibaraki 305-8573, Japan
Email: sakai@kz.tsukuba.ac.jp
[5)] National Institute for Land and Infrastructure Management, Ministry of Land, Infrastructure and Transport, Ibaraki 305-0802, Japan, Email: suwada-h92h9@nilim.go.jp
[6)] Building Research Institute, Ibaraki 305-0802, Japan
Email: fukuyama@kenken.go.jp

ABSTRACT

To establish a simple and cost effective testing technique to investigate seismic behaviors of RC structures, extremely small scaled model structures consisting of high performance fiber reinforced cement composite (HPFRCC) material reinforced only with longitudinal reinforcement are fabricated, and their dynamic behaviors are experimentally and analytically investigated.

INTRODUCTION

Shaking table tests have been widely applied to investigate dynamic behaviors of structures under earthquake excitations. In the shaking table tests of reinforced concrete (R/C) structures, relatively large specimens are generally tested to eliminate difficulties in fabricating specimens. However, the number of shaking table that have enough capacity to carry out large-scale tests are limited, and the experiments are generally costly and more time is required. Even when shaking table tests using relatively small specimen are carried out, it may be difficult to completely reproduce scaled specimens using scaled materials. Therefore another methodology is needed to carry out cost effective shaking table tests.

Recently, high performance fiber reinforced cement composite (HPFRCC) has been developed. The HPFRCC, which is mortar matrix mixed with fibers, has several special characteristics including tension stiffening after cracking, multiple cracking effects etc. Since its behavior is similar to that of normal concrete confined with shear reinforcement, the HPFRCC can be the candidate material for simple dynamic tests using small-scaled RC models.

The objective of this research is to establish a simple and cost effective testing technique to investigate seismic behaviors of RC structures. To this end, extremely small-scaled models (approximately 1/20 scaled model) consisting of only HPFRCC and longitudinal reinforcement are designed and fabricated, and their behaviors are investigated by shaking table tests and fiber model analyses. The results show that the proposed models have ductile behaviors with spindle shaped hysteretic loops of typical RC members and that their responses can be numerically simulated considering strain rate effects.

TEST SPECIMENS

The extremely small-scaled column specimens investigated in this study are not the simply size-reduced models of existing full-scale R/C members but those consisting of longitudinal steel reinforcement and HPFRCC

material without lateral reinforcement.

The HPFRCC used in specimens is mortar matrix (water-cement ratio: 45%, sand-cement ratio: 40%) mixed with 1.0% volume ratio of polyethylene fiber (fiber length: 15mm, the diameter of a fiber: 12 μm). Two types of specimens are designed as follows: Type-S (stub) specimen with a stub at each end and Type-P (plate) specimen with a plate at each end. The dimension of specimens is shown in Figure 1. Each specimen has a cross section of 30 x 30 mm and the height h of 180 mm. The shear-span-to-depth ratio of each specimen is 3.0, and the tensile reinforcement ratio is 2.19%. Tables 1 and 2 show the mechanical properties of HPFRCC and longitudinal reinforcement obtained by the static material tests.

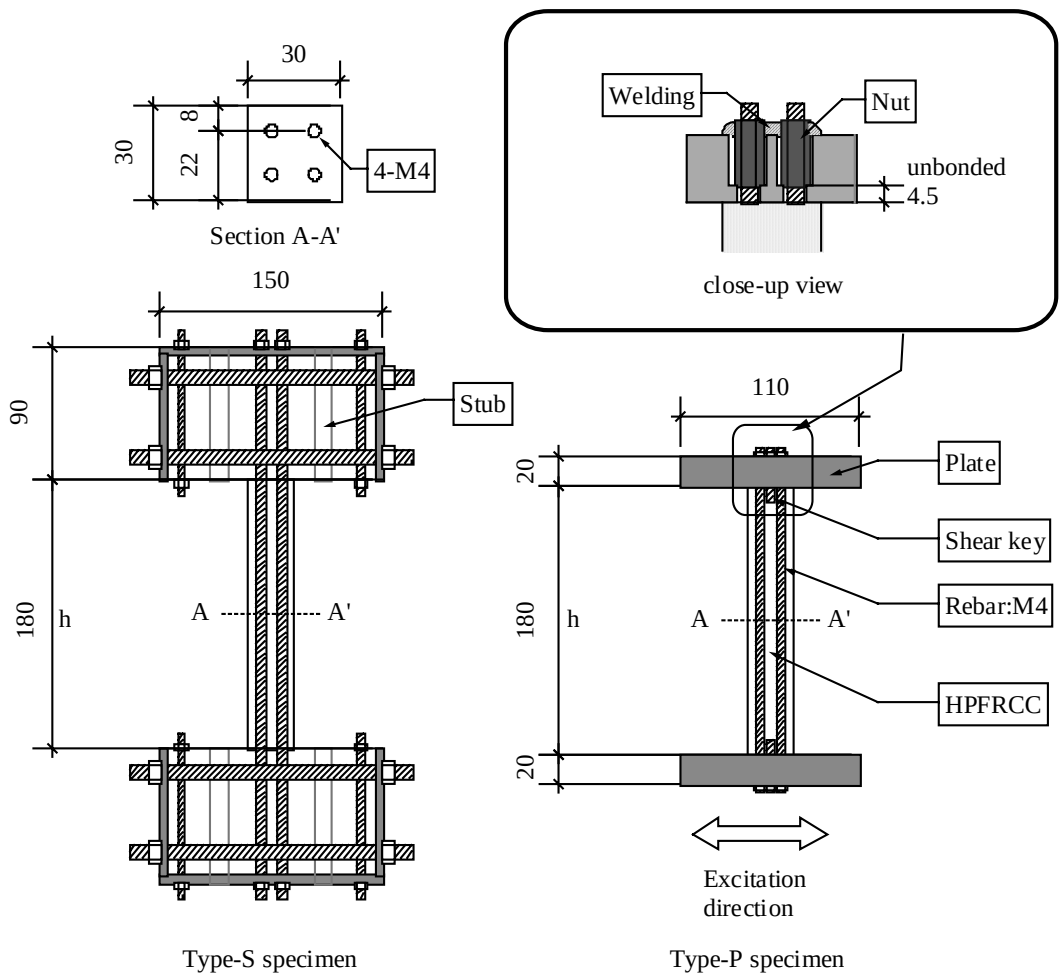

Figure 1. Dimension of Specimens

Table 1. Mechanical Properties of HPFRCC (obtained from static material test)

Specimen	Age (days)	Young's Modulus*1 E_c (N/mm^2)	Compressive Strength σ_B (N/mm^2)	Strain at Compressive Strength ε_B (%)	Tensile Strength σ_t (N/mm^2)	Strain at Ultimate Tensile Strength ε_{ut} (%)
Type-S	19	1.95×10^4	45.74	0.34	2.00	$\geqq 2.0^{1)}$
Type-P	18	1.69×10^4	47.68	0.40	2.14	

*1 secant modulus at 1/3 σ_B

*2 average of 3 cylinders

Table 2. Mechanical Properties of Longitudinal Reinforcement (obtained from static material test)

	Section Area (mm^2)	Young's Modulus E_s (N/mm^2)	Yield Strength *1 σ_y (N/mm^2)	Yield Strain ε_y (%)
M4	9.87	1.35×10^5	443.77	0.55

*1 0.2% off-set value

*2 average of 3 test pieces

SHAKING TABLE TEST

Test Setup

The excitation system is shown in Figure 2. Each specimen is placed on and fixed to component (c). This system has horizontal and vertical sliders, which enable specimens to deform in the lateral and axial direction when they are subjected to anti-symmetric bending during excitations.

The relative displacement y between point (a) and component (c) is measured in the direction of excitation. Accelerometers are installed at point (a), (d), and the shaking table. Load cells (1) and (2) are installed at both ends of the component (c), which is placed on horizontal sliders, to directly evaluate the inertia force acting on the specimen. The inertia force Q of each specimen is calculated from Eqs. (1) and (2) based on the measured force shown in Figure 3.

$$\boldsymbol{Q} - \boldsymbol{P_I} + \left(- \boldsymbol{P_{L1}} - \boldsymbol{P_{L2}} - \boldsymbol{P_{DS}}\right) = 0 \tag{1}$$

Assuming $\boldsymbol{P_{DS}} \approx 0$

$$\boldsymbol{Q} \approx \left(\boldsymbol{P_{L1}} + \boldsymbol{P_{L2}}\right) + \boldsymbol{P_I} \tag{2}$$

$$\boldsymbol{P_I} = \boldsymbol{m} \cdot \boldsymbol{a}$$

where P_{L1} and P_{L2} are the forces measured with load cells (1) and (2), respectively, P_I is the inertia force acting on lower stub and component (c), and m and a are their mass and absolute acceleration, respectively.

To observe the effects of different design details at specimen ends, i.e., stub end and plate end, the rotation angle $\theta_{h'}$ at 10mm above the column base is measured as shown in Figure 4. The data are recorded with a sampling interval of 1/500 sec.

Test Program

In this experiment, the gross weight W of a specimen including self-weight and equipment weight is 3234N. The calculated initial period of the specimen is 0.074 seconds. The sine wave of which amplitude increases gradually as shown in Figure 5 is used to excite specimens. The period of the sine wave is 0.20 seconds, which is about 3 times of the calculated period of specimens.

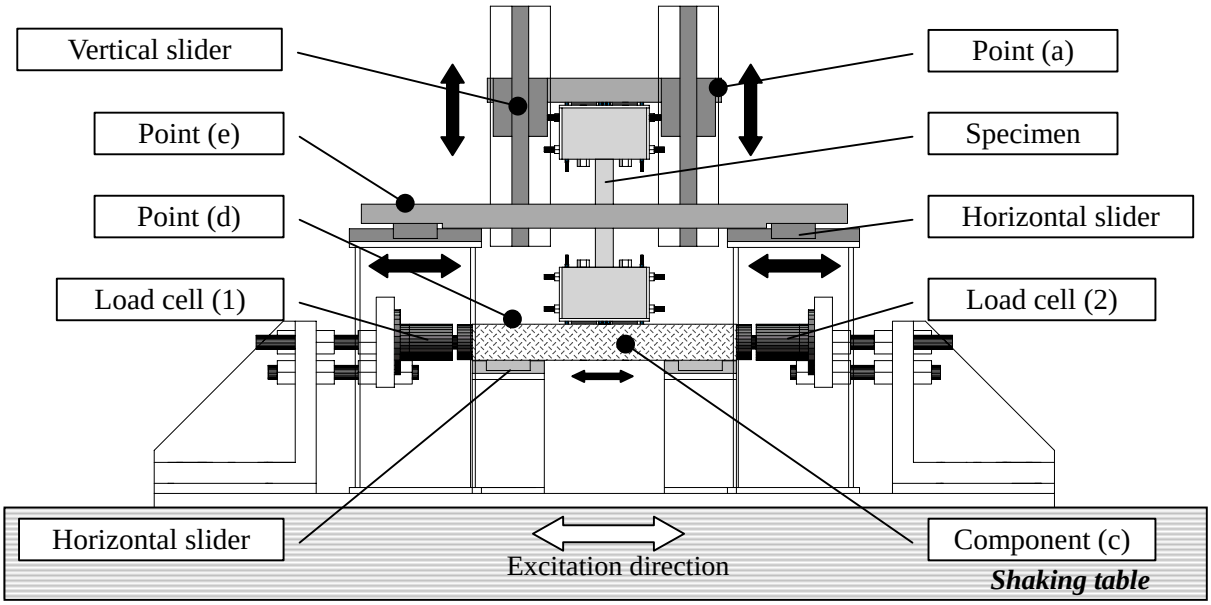

Figure 2. Excitation System

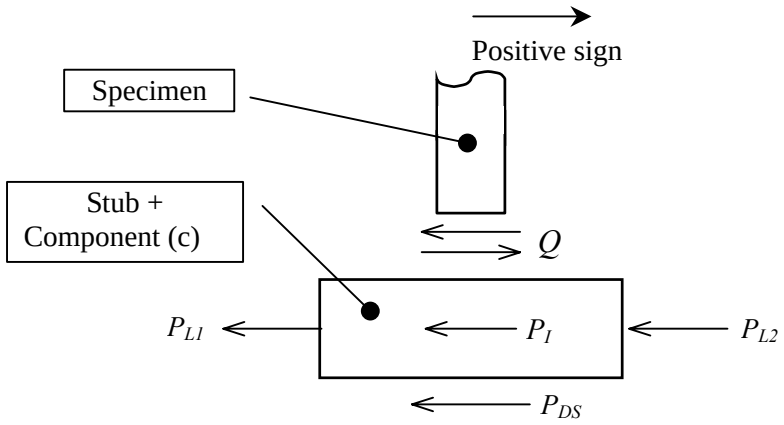

Q: inertia force of specimen
(restoring and damping force)
P_{L1}: force obtained from load cell (1)
P_{L2}: force obtained from load cell (2)
P_I: inertia force of stub and component (c)
P_{DS}: damping force from slider

Figure 3. Inertia Force of Specimen and Measured Force

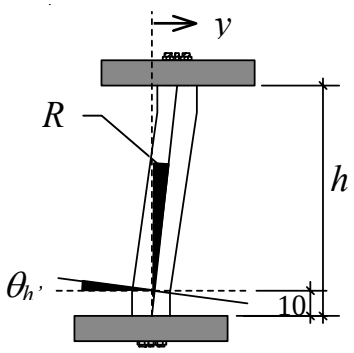

Figure 4. Rotation Angle Measurement

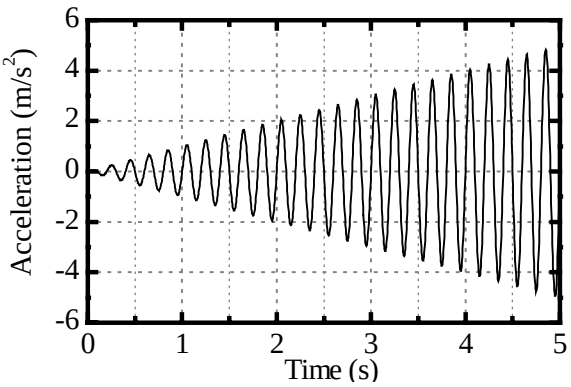

Figure 5. Input Sine Wave

Test Results

Figure 6 shows the relationship of response shear coefficient C (= Q / W) and drift angle R (= y / h) of each specimen. Both specimens show ductile behaviors with spindle shaped hysteretic loops. To compare the fundamental characteristics of extremely small-scaled specimens proposed herein to those of regular R/C members, the following two parameters α_y and β are calculated in Table 3. They are defined as:

(1) α_y: the ratio of secant stiffness at yielding to the initial stiffness
(2) β: the ratio of post-peak stiffness to the initial stiffness

The yielding of the specimen is defined as the point where its instant stiffness is lower than 10% of the initial stiffness. As can be found in Table 3, these values successfully simulate those of R/C members.
Figure 7 shows the $\theta_{h'}$ - R relationship of both specimens. This figure shows that the ratio of $\theta_{h'}$ of Type-P specimen to that of Type-S specimen lies in the range of 1.5 to 2.0, and the deformation is more significantly concentrated over the end regions for Type-P specimen.

The maximum Q value (Q_{MAX}) of Type-S specimen during shaking table test is 20% larger than that of Type-P specimen although they have the same sectional and material properties. To understand the reason of different Q_{MAX} values, fiber model analyses of both specimens are carried out and their fundamental behaviors are carefully investigated.

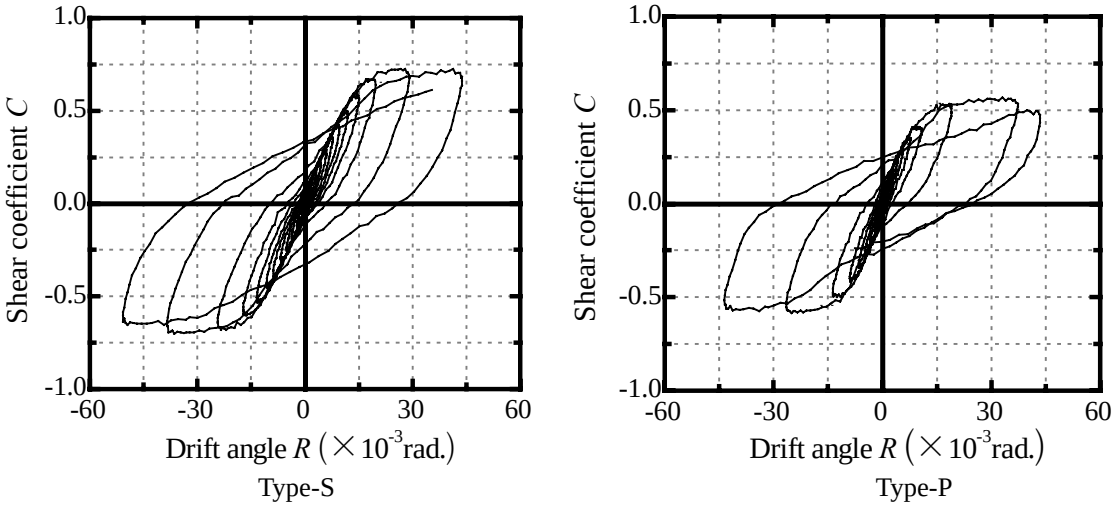

Figure 6. Shaking Table Test Results

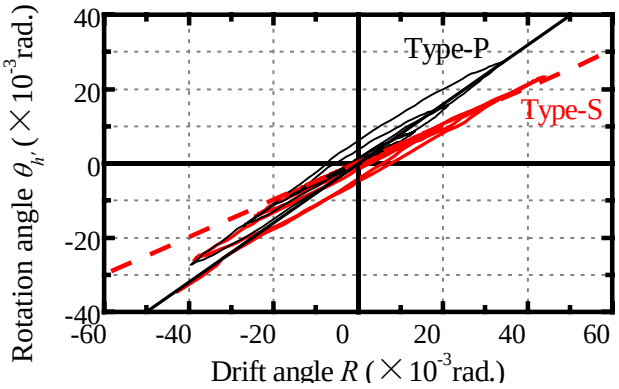

Figure 7. $\theta_{h'}$ - R Relationship

Table 3. Degradation in Stiffness

	α_y	β
Type-S specimen	0.25	0.040
Type-P specimen	0.23	0.033

FIBER MODEL ANALYSIS CONSIDERING STRAIN RATE EFFECTS

To investigate the difference in Q_{MAX} due to design details at specimen ends and strain rate effects, fiber model analyses are carried out.

Assumptions in Computation

Curvature Distributions

Figure 8 shows the curvature distributions assumed in the analysis. As can be found in the figure, a triangular curvature distribution is assumed for Type-S specimens, while a combined profile of rectangular and triangular distribution is assumed for Type-P specimen since the longitudinal reinforcement is unbonded to HPFRCC over the length of h_p in the end plates as shown in Figure 1.

The curvature ${}_s\phi_0$ at the critical section of Type-S specimen at a given displacement ${}_sy$, and the rotation angle ${}_s\theta_{h'}$ at h' (=10 mm) above the column base, is determined by Eqs. (3) and (4), respectively, assuming the curvature distribution shown in Figure 8(a).

$$ {}_s\phi_0 = \frac{3\cdot {}_s y}{h^2} \tag{3} $$

$$ {}_s\theta_{h'} = \frac{1}{2}{}_s\phi_0 \cdot h'\left(2-\frac{h'}{h}\right) = \frac{3}{2}\frac{{}_s y}{h}\cdot\frac{h'}{h}\left(2-\frac{h'}{h}\right) \tag{4} $$

The curvature at the critical section of Type - P specimen, ${}_p\phi_0$, is determined as follows. Based on the curvature distribution of Type-P specimen shown in Figure 8(b), the drift ${}_py$ and the rotation angle ${}_p\theta_{h'}$ at a distance of h' (=10 mm) from the bottom stub are obtained as Eqs. (5) and (6).

$$ {}_P y = \frac{1}{3} {}_p\phi_0 h^2 + {}_p\phi_{hp} \cdot h_p \left(h + \frac{h_p}{2} \right) \tag{5} $$

$$ {}_P\theta_{h'} = \frac{1}{2} {}_p\phi_0 \cdot h' \left(2 - \frac{h'}{h} \right) + {}_p\phi_{hp} \cdot h_p \tag{6} $$

Where ${}_p\phi_0$ and ${}_p\phi_{hp}$ are curvatures at critical section and at h_p below the end plate, respectively. Considering the experimental results shown in Figure 7, the relation of ${}_p\theta_{h'}$ and ${}_s\theta_{h'}$ is assumed as Eq. (7).

$$ {}_P\theta_{h'} = 2\ {}_S\theta_{h'} \tag{7} $$

Setting ${}_py$ of Eq.(5) equal to ${}_sy$ of Eq.(3), the curvature ${}_p\phi_0$ at critical section at a given displacement ${}_py$ (=${}_sy$) is obtained from Eqs. (4) through (7). The location of the neutral axis and the strain of each fiber segment are then determined based on the curvature at critical section ${}_s\phi_0$ (or ${}_p\phi_0$) obtained above, the equilibrium condition of axial force of a section and the plane section assumption.

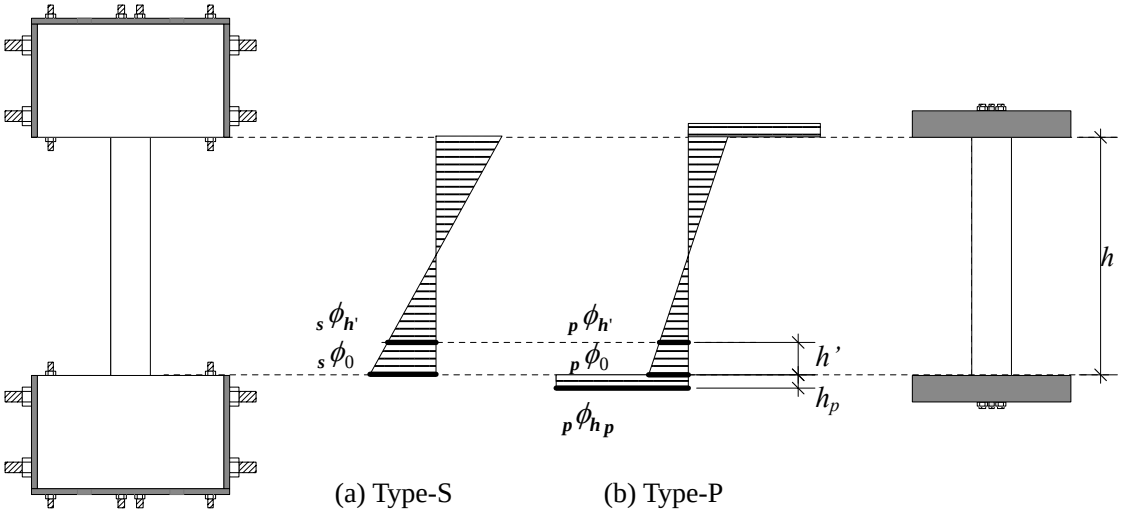

(a) Type-S (b) Type-P

Figure 8. Curvature Distribution

Material Characteristics

To consider strain rate effects on the σ - ε relationship on material characteristics basis, the strain rate ${}_k\dot{\varepsilon}$ is calculated by Eq. (8).

$$ {}_k\dot{\varepsilon} = \Delta_k \varepsilon / \Delta t \tag{8} $$

Where $\Delta_k\varepsilon$ and Δt are the strain increment of element k and the time increment, respectively.

Figure 9 shows material properties model for HPFRCC and longitudinal reinforcement.

In compression, the σ - ε relation of HPFRCC is represented with (1) a linear line having a slope of initial Young's modulus E_c, (2) a parabola curve that passes through the origin (0, 0) and the peak (ε_B, σ_B), (3) a linearly falling branch and (4) a residual strength plateau with $0.5\sigma_B$. In tension, a tensile strength of $\sigma_B/20$ after yielding is assumed up to 2% for Type-S specimen, while the strength contribution is neglected for Type-P specimen. The Young's modulus E_c and strength σ_B shown in Table 1 is factored in accordance with strain rate, as shown in Eqs. (9) through (12).

In both tension and compression, the $\sigma - \varepsilon$ relation of longitudinal reinforcement is represented with (1) a linear line having initial Young's modulus *Es* and (2) a linear line with 1/100 E_s. The yield strength σ_y show in Table 2 is factored in accordance with strain rate, as shown in Eq. (13).

HPFRCC

Young's Modulus

$$|\dot{\varepsilon}| > 10^1 \mu/\sec$$
$$ {}_d\boldsymbol{E}_c = \left(0.02 \cdot \log|\dot{\varepsilon}| + 0.98\right) \cdot {}_s\boldsymbol{E}_c \qquad (9)$$
$$|\dot{\varepsilon}| \le 10^1 \mu/\sec$$
$$ {}_d\boldsymbol{E}_c = {}_s\boldsymbol{E}_c$$

Where, ${}_d\boldsymbol{E}_c$: Young's modulus of HPFRCC (dynamic)

${}_s\boldsymbol{E}_c$: Young's modulus of HPFRCC (static)

Compressive Strength

$$|\dot{\varepsilon}| > 10^1 \mu/\sec$$
$$ {}_d\sigma_B = \left(0.06 \cdot \log|\dot{\varepsilon}| + 0.94\right) \cdot {}_s\sigma_B \qquad (10)$$
$$|\dot{\varepsilon}| \le 10^1 \mu/\sec$$
$$ {}_d\sigma_B = {}_s\sigma_B$$

Where, ${}_d\sigma_B$: Compressive strength of HPFRCC (dynamic)

${}_s\sigma_B$: Compressive strength of HPFRCC (static)

Tensile Strength

· Type-S

$$\sigma_t = \sigma_B / 20 \quad (\sigma_B = {}_s\sigma_B \text{ or } {}_d\sigma_B) \qquad (11)$$

· Type-P

$$\sigma_t = 0 \qquad (12)$$

Longitudinal Reinforcement

Yield Strength of Longitudinal Reinforcement

$$|\dot{\varepsilon}| > 10^2 \mu/\sec$$
$$ {}_d\boldsymbol{f}_y = \left(0.05 \cdot \log|\dot{\varepsilon}| + 0.90\right) \cdot {}_s\boldsymbol{f}_y \qquad (13)$$
$$|\dot{\varepsilon}| \le 10^2 \mu/\sec$$
$$ {}_d\boldsymbol{f}_y = {}_s\boldsymbol{f}_y$$

Where, ${}_d\boldsymbol{f}_y$: Yield strength of longitudinal reinforcement (dynamic)

${}_s\boldsymbol{f}_y$: Yield strength of longitudinal reinforcement (static)

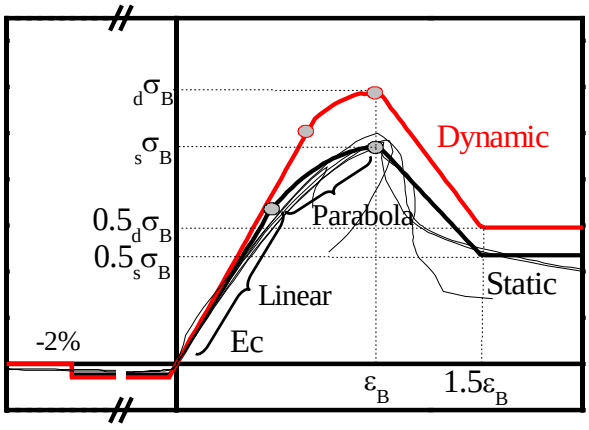

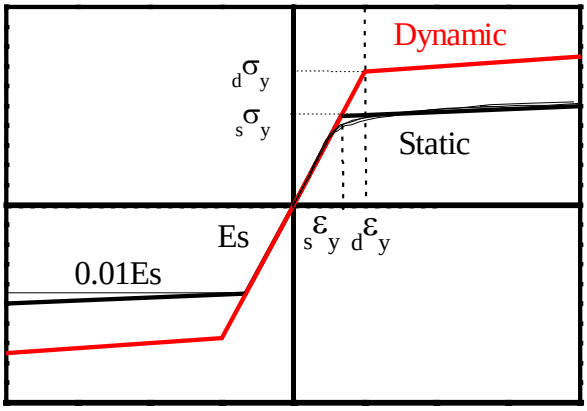

${}_s\sigma_B = 47(\boldsymbol{N}/\boldsymbol{mm}^2)$, ${}_s\varepsilon_B = 0.4(\%)$

$\boldsymbol{E}_c = 1.8 \times 10^4 (\boldsymbol{N}/\boldsymbol{mm}^2)$

HPFRCC

${}_s\sigma_y = 450(\boldsymbol{N}/\boldsymbol{mm}^2)$

$\boldsymbol{E}_s = 1.35 \times 10^5 (\boldsymbol{N}/\boldsymbol{mm}^2)$

Longitudinal Reinforcement

Figure 9. Model of Material Properties

Results and Discussions

Computed results are compared with shaking table test results in Figure 10. Figure 11 shows the strain rate and its corresponding magnification factor of tensile reinforcement at the critical section of each specimen obtained in the computation. The computed Q_{MAX} of Type-S specimen subjected to dynamic loading agrees well with the test result considering the strain rate effects. The strain rate and corresponding magnification factor of material strength is, as shown in Figure 11, generally lower in Type-P specimen, which is attributed to a curvature profile different from that assumed for Type-S specimen. Although the computed Q_{MAX} of Type-P specimen is accordingly lower than that of Type-S specimen, it is still higher by 15% than experimental results.

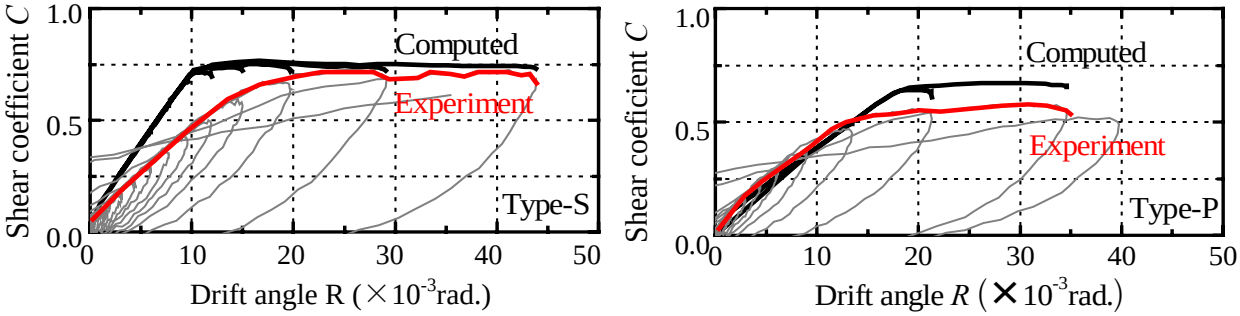

Figure 10. Comparison of Computed Results with Dynamic Test Result

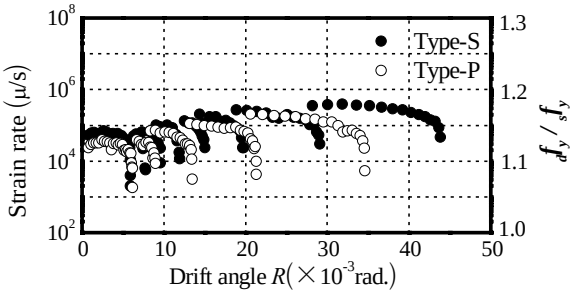

Figure 11. Computed Strain Rate of Tensile Reinforcement

CONCLUSION

To establish a simple and cost effective testing technique to simulate seismic behaviors of R/C structures, extremely small-scaled model structures consisting of high performance fiber reinforced cement composite (HPFRCC) material reinforced only with longitudinal reinforcement are fabricated, and their behaviors are experimentally and analytically investigated.

1) The specimens which are investigated in this study show ductile behaviors with spindle shaped hysteretic loops. The ratio of secant stiffness at yielding to the initial stiffness (α_y) and that of post-peak stiffness to the initial stiffness (β) also successfully simulates those of typical R/C members.
2) The rotational angle $\theta_{h'}$ of column is measured at a distance of 10 mm from its base, and compared in both specimens. The results show that the angle $\theta_{h'}$ of Type-P specimen is 1.5 to 2.0 times of that of Type-S specimen at the same drift angle. This is primarily due to the presence of longitudinal reinforcement unbonded to HPFRCC, and highly contributing to the concentrated deformation over the end region of Type-P specimen.
3) The maximum inertia force Q_{MAX} of Type-S specimen observed during shaking table test is 20% larger than that of Type-P specimen although they have the same sectional and material properties. The computed Q_{MAX} of Type-S specimen subjected to dynamic loading agrees well with the experimental result considering the strain rate effects. The computed Q_{MAX} of Type-P specimen, however, is about 15% higher than the experimental result. This result may be attributed to the overestimated strain rate effect in Type-P specimen, and the relation between the design detail at the unbonded region and strain rate effect needs to be clarified.

REFERENCES

1) Sato, Y., Fukuyama, H., Suwada, H. (2001) "A Proposal of Tension-Compression Cyclic Loading Test Method for Ductile Cementitious Composite Materials." *Journal of Structural and Construction Engineering*, No.539, pp. 7-12 (in Japanese).
2) Hosoya, H., Okada, T., Kitagawa, Y., Nakano, Y., Kumazawa, F. (1996) "Fiber Model Analysis of Reinforced Concrete Members with Consideration of The Strain Rate Effect." *Journal of Structural and Construction Engineering*, No.482, pp. 83-92 (in Japanese).